A Technique for Quantifying Wrist Motion Using Four-Dimensional Computed Tomography: Approach and Validation

Kristin Zhao[1]
Rehabilitation Medicine Research Center,
Department of Physical Medicine and Rehabilitation,
Mayo Clinic,
200 First Street SW,
Rochester, MN 55905
e-mail: zhao.kristin@mayo.edu

Ryan Breighner
Biomechanics Laboratory,
Division of Orthopedic Research,
Mayo Clinic,
200 First Street SW,
Rochester, MN 55905
e-mail: Breighner.Ryan@mayo.edu

David Holmes III
Department of Physiology and Biomedical Engineering,
Mayo Clinic,
200 First Street SW,
Rochester, MN 55905
e-mail: Holmes.David3@mayo.edu

Shuai Leng
Department of Radiology,
Mayo Clinic,
200 First Street SW,
Rochester, MN 55905
e-mail: Leng.Shuai@mayo.edu

Cynthia McCollough
Department of Radiology,
Mayo Clinic,
200 First Street SW,
Rochester, MN 55905
e-mail: mccollough.cynthia@mayo.edu

Kai-Nan An
Fellow ASME Biomechanics Laboratory,
Division of Orthopedic Research,
Mayo Clinic,
200 First Street SW,
Rochester, MN 55905
e-mail: an.kainan@mayo.edu

Accurate quantification of subtle wrist motion changes resulting from ligament injuries is crucial for diagnosis and prescription of the most effective interventions for preventing progression to osteoarthritis. Current imaging techniques are unable to detect injuries reliably and are static in nature, thereby capturing bone position information rather than motion which is indicative of ligament injury. A recently developed technique, 4D (three dimensions + time) computed tomography (CT) enables three-dimensional volume sequences to be obtained during wrist motion. The next step in successful clinical implementation of the tool is quantification and validation of imaging biomarkers obtained from the four-dimensional computed tomography (4DCT) image sequences. Measures of bone motion and joint proximities are obtained by: segmenting bone volumes in each frame of the dynamic sequence, registering their positions relative to a known static posture, and generating surface polygonal meshes from which minimum distance (proximity) measures can be quantified. Method accuracy was assessed during in vitro simulated wrist movement by comparing a fiducial bead-based determination of bone orientation to a bone-based approach. The reported errors for the 4DCT technique were: 0.00–0.68 deg in rotation; 0.02–0.30 mm in translation. Results are on the order of the reported accuracy of other image-based kinematic techniques.
[DOI: 10.1115/1.4030405]

Keywords: carpal kinematics, dynamic CT imaging

Introduction

The wrist joint is an articulation consisting of many bones and ligamentous structures which, during normal function, allows complex motions while still maintaining stability. The wrist is the most frequently injured upper extremity joint, with wrist ligament injuries being subject to a high rate of misdiagnosis [1–3]. Accurate diagnosis is crucial for providing the most effective interventions that, if not implemented early enough, can lead to significant pain and suffering for patients and limit the spectrum of treatment options [4–8]. Magnetic resonance imaging (MRI) cannot accurately detect rupture of the scapholunate interosseous ligament [9,10]. Further, since standard MRI and CT imaging are static in nature, only abnormal carpal bone position can be detected, without the possibility to analyze abnormal motion. These dynamic changes can be assessed occasionally with fluoroscopy [11–13], but more commonly, especially in patients with mild or early injuries, a definitive diagnosis is made during surgery.

Prior investigations of carpal motion have focused on understanding normal and pathological motion patterns in vitro and in vivo. Considerable knowledge has been gained about basic biomechanics of wrist function including carpal bone motion [14–25], the effect of ligamentous constraints [26–33], and bilateral symmetry [17,34,35]. However, these studies have been limited by their inability to capture dynamic four-dimensional (4D) (three spatial dimensions + time) data during unconstrained movements in vivo. Recently, our research team and others [36–44] have noted the utility of four-dimensional (4D) CT image sequences as a visualization and clinical tool for assessing dynamic movements in various joints. 4DCT is an imaging technique whereby joint motion is acquired using a dynamic sequential scanning mode similar to CT perfusion. In this mode, images of a moving joint are continuously acquired. Therefore, it holds promise to detect injuries earlier when only subtle bony motion changes are occurring. Due to the complex geometry and motions, this data are best viewed volumetrically. Volume-rendered dynamic image sequences can be rotated and viewed with varying bone opacities to assist in clinical decision-making.

The next step in successful clinical implementation of the tool is quantification and validation of measures from the 4DCT image sequences that will enable selection of appropriate and timely interventions for these patients. This includes quantification of measures that we call imaging biomarkers, including joint proximity which approximates the articular joint contact which is known to be affected by wrist instability and osteoarthritis. The purpose of this manuscript is to describe a 4DCT approach for quantifying wrist motion and validate the accuracy in two

[1]Corresponding author.
Manuscript received September 9, 2014; final manuscript received April 12, 2015; published online June 3, 2015. Assoc. Editor: Zong-Ming Li.

cadaveric specimens during motion induced using an in vitro wrist simulator.

Methods

4DCT Imaging Technique. The 4DCT technique is described in more detail in our previous manuscript [44], but a brief overview is presented here. Initially, static CT scans are obtained of the distal forearm and hand using a routine wrist scan protocol, with 120 kV, 200 effective mAs, 1 s rotation time, and helical pitch of 1. A dual-source CT scanner (Definition Flash, Siemens Healthcare, Forchheim, Germany) is utilized, consisting of two independent X-ray tubes and detector arrays mounted onto a rotating gantry at a 94 deg offset from one another. A dynamic sequential scanning mode similar to CT perfusion is used. In this mode, images of a moving joint are continuously acquired without table translation. Two seconds of data are acquired for each movement (full cycle of flexion–extension and radial–ulnar deviation). Scan parameters include 0.28 s gantry rotation, $2 \times 64 \times 0.6$ mm detector collimation (38.4 mm z-axis coverage), 120 kV, and 100 mAs per rotation. These parameters make the approach suitable for joints occupying relatively small volumes. Image volumes (Fig. 1) are reconstructed at each of 18 time points over the 2 s cycle (i.e., 9 Hz sampling rate). Images are output in digital imaging and communications in medicine (DICOM) format for determination of metrics and imaging biomarkers. Dose-reduction strategies were finalized previously [44]. For each 4DCT scan, the volume CT dose index (CTDIvol) is approximately 36 mGy, which is approximately three times that of the static wrist CT scan reported in the literature [45]. The effective dose for the reported static wrist CT was 0.03 mSv; the effective dose of the 4DCT dose is estimated to be 0.09 mSv, which is only a very small fraction (3%) of the average annual background radiation in the U.S. (3 mSv) [46].

Image Analysis. Mayo Clinic Analyze (Rochester, MN) was used for image segmentation and mesh generation; Matlab (Natick, MA) was used for surface registration and proximity calculations. Image analysis was demonstrated on the scapholunate joint, requiring segmentation of the scaphoid, lunate, and radius. Multiple bone segmentation of the wrist is quite challenging due to the thin cortical bone, partial volume effects, and bone-to-bone proximity [47]. A combination of user-driven tools was developed to address this issue. Global thresholding of the entire carpus initialized the segmentation process, and a standard graph-based connected component algorithm was used to separate and label each bone [48]. When necessary, segmentation was aided by geodesic splitting. Geodesic skeleton by influence zone is a morphologic technique to separate two binary objects from two seed points [49]. Repeated application of geodesic splitting can extract each bone from the bone group.

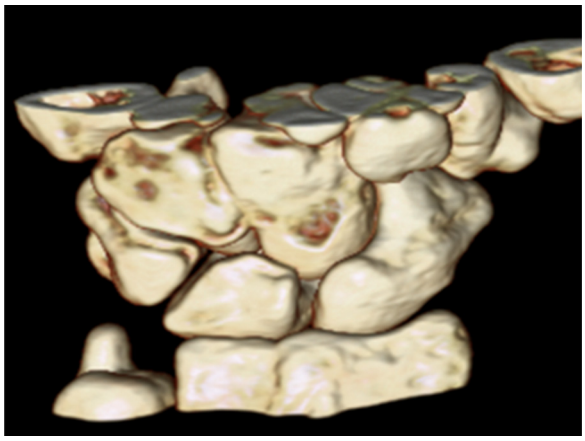

Fig. 1 A single three-dimensional volume-rendered image volume from a 4DCT image sequence (high resolution, not shown). Image volumes are reconstructed at each of 18 time points over the 2 s movement cycles. Images are output in DICOM format for determination of metrics and imaging biomarkers.

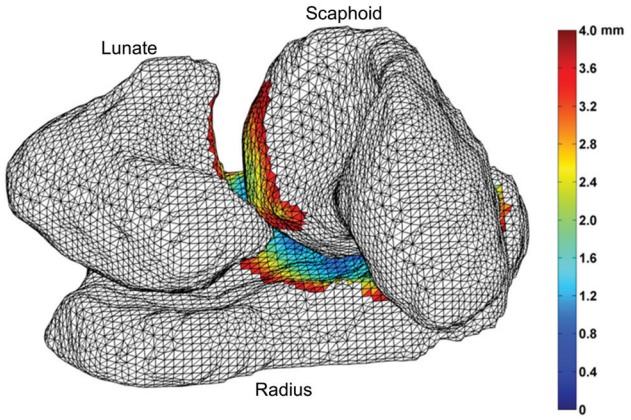

Fig. 2 Proximity values represented on the scaphoid, lunate, and radius articulating surfaces of a right wrist at one time point (from the 18 total) of a 4DCT sequence (palmar view). Proximity values are calculated as the minimum distance from all mesh vertices on the first surface mesh to the second bone mesh. The resulting proximity maps are depicted as a contour color map indicating the minimum distances between the articulating bone surfaces.

Following segmentation, polygonal meshes were generated from the segmented bone data for use in registration and proximity measurements. After surfaces were reconstructed using conventional marching cubes [50], an adaptive deformation approach was applied to improve the efficiency of the mesh representations [51]. This technique has previously been validated in several applications [52,53].

Registration of the surface meshes (alignment of the bone surfaces from the static scan to those from 4DCT) was achieved using the iterative closest points matching algorithm [54]. This algorithm determines the rotation and translation that minimize the

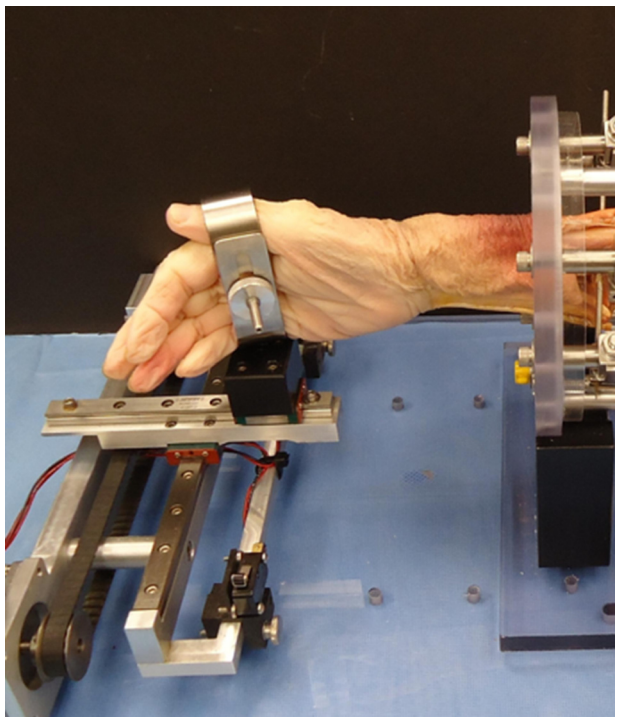

Fig. 3 Custom CT-compatible cadaveric wrist simulator for simulating wrist flexion/extension and radial/ulnar deviation motions via a linear motor (fiducial markers not shown)

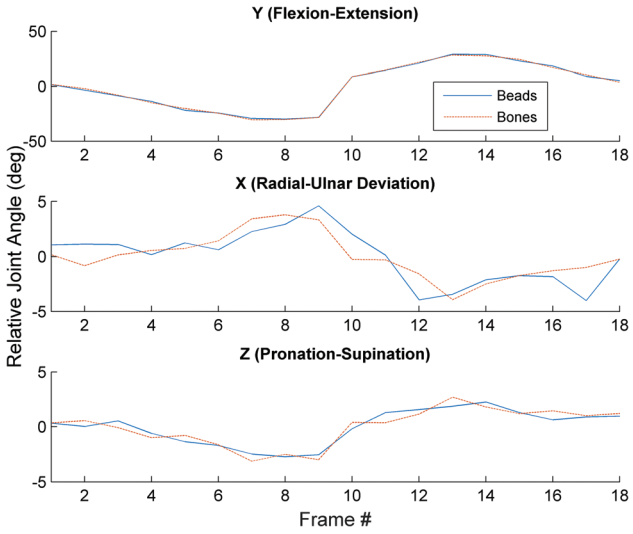

Fig. 4 Time series data of bead-based and bone-based rotation values of the scaphoid during a wrist flexion–extension trial

distances between points in two point clouds, i.e., the vertices of the surface meshes. The geometries of the radius, scaphoid, and lunate were sufficiently distinct, enabling the algorithm to achieve registration and avoid extraneous local minima in lieu of any manual initial guess as to the bone orientations/locations.

Proximity values were then determined for the lunate and radius articular surfaces for all volumes of the dynamic sequences and were defined as the minimum distance from all mesh vertices on the lunate (and radius, separately) to the scaphoid bone mesh. The resulting proximity values are depicted as a contour color map indicating the minimum distances between the articulating subchondral bone surfaces (Fig. 2).

Experimental Setup. To determine the accuracy of 4DCT imaging for kinematic measurements, dynamic evaluations of two cadaveric wrists were performed. For intact wrist motion evaluation, the hand/wrist specimen's distal radius and ulna were fixed to a custom wrist simulator (Fig. 3), and custom four-bead fiducial clusters (not shown) were rigidly attached to the radius, scaphoid, and lunate through skin incisions and oriented such that they would not interfere with carpal bone motion during wrist movement. Teflon beads were used to prevent artifacts in the 4DCT images. The specimens were oriented such that the long axis of the radius aligned with the long axis (through the bore) of the CT scanner. One trial each of flexion–extension and radial—ulnar deviation was simulated in two cadaveric specimens by actuation of the metacarpals (Fig. 3). 4DCT image sequences were obtained such that one full motion cycle was collected in 2 s; this speed replicated an approximate average wrist velocity of 50 deg/s, as observed in the workplace [55].

Data Analysis. Eighteen image volumes were obtained for each wrist movement, and techniques described above were used to segment the beads and bony anatomy (radius, scaphoid, and lunate) from the images. To establish the quality of the fiducial beads as a gold standard, fiducial localization error was assessed as the RMS of distances between homologous beads in both the 4D and static CT scans. Registration accuracy was quantified using the determined relative orientations of fiducial bead sets attached to the scaphoid and lunate and the respective bone-based orientation. Registration errors were calculated as the relative transformations from the global transformation aligning the fiducials, to the global transformations aligning the bones, from each volume of the 4DCT to the transformed static bead locations (after applying the transformations obtained during registration). Values were expressed in the global (scanner) coordinate system. Additionally, distances between homologous points on the bones surfaces aligned using the bead-based and bone-based registrations were calculated to provide an estimate of the upper bound on surface alignment for potential interosseous proximity calculations. These represent an estimate of the error in calculating interosseous proximities from the entire analysis process.

Results

Representative time series data of bead-based and bone-based rotation values of the scaphoid during a flexion–extension trial can be found in Fig. 4. The rotation range of motion was 20.0–60.0 deg about the primary axis of motion for the scaphoid and lunate; rotation about the tertiary axes ranged from 2.0 to 9.0 deg. Translations of the bone centroids about the three axes ranged from 2.0 to 11.0 mm. Mean fiducial localization error values were small, 0.054 (0.018) mm, with a range of 0.023–0.139 mm, indicating that the fiducials (beads) were reliably locatable in the image sets. The maximum distances between homologous points on the coregistered lunate, radius, and scaphoid meshes (aggregating acquisition, segmentation, surface reconstruction, and registration errors) were 0.943, 0.418.0.376 mm, respectively. Mean and standard deviation values for angular and translational errors for each bone are shown in Table 1. The reported errors for the 4DCT technique are on the order of the reported accuracy of other static and dynamic image-based kinematic techniques [56–59].

Discussion

This study describes the 4DCT approach for quantifying wrist motion in two cadavers and establishes an accuracy that is on the order of other static and dynamic imaging approaches for image-based kinematic techniques. The advantage of the 4DCT approach is in its dynamic, tomographic data sets which enable the quantification of measures which approximate joint contact (i.e., joint proximity) that are known to be affected by wrist instability and osteoarthritis. Further, the dynamic nature of the scanning technique enables proprioceptive and inertial influences on movement to be captured throughout the 18 volumes.

The power of the 4DCT approach lies in its potential for impact on clinical care for patients with scapholunate ligament injuries, among other pathologies. If the approach, including determination of biomarkers, allows detection of injuries earlier when only subtle bony motion changes are occurring, appropriate and timely surgical or conservative interventions strategies can be prescribed. This improvement in care will be possible due to the dynamic nature of the imaging technique, as current static techniques (including MR and CT) can only detect abnormal bone positions. Abnormal bone positions are indicative of extreme or end-stage instability; our approach has the potential to prescribe early

Table 1 Mean (SD) values for angular and translational errors for each bone

	Rotation (deg)			Translation (mm)		
	X	*Y*	*Z*	*X*	*Y*	*Z*
Lunate	−0.002 (1.807)	−0.679 (1.150)	−0.538 (0.770)	−0.105 (0.282)	0.086 (0.201)	0.298 (0.380)
Radius	−0.137 (0.550)	0.314 (0.563)	−0.034 (0.334)	0.020 (0.106)	0.041 (0.103)	−0.132 (0.230)
Scaphoid	−0.224 (0.822)	0.400 (0.893)	0.046 (0.601)	−0.011 (0.127)	−0.020 (0.125)	0.038 (0.216)

interventions, thereby preventing eventual progression to osteoarthritis.

Limitations. The limitations of the described 4DCT approach as compared to other imaging approaches include the smaller field of view, which allows the acquisition of motion in joints that require smaller image volumes. Further, the 75 ms temporal resolution of image volumes limits the movement velocity for acquisition; however, movements typically used during daily activity and the workplace can be described [55]. Finally, the accuracy of kinematics and proximity-based measures are affected by segmentation and registration accuracy, which have been fully described. However, to the best of our knowledge there are no methods with sufficient resolution to allow insight into the accuracy of our image-based measures of proximity.

Conclusion

Existing diagnostic tools are unable to acquire dynamic, three-dimensional information during carpal bone motion. Even the most recent advances with MR arthrography lack good correlation with wrist arthroscopy [60]. The proposed approach is accurate, available on clinical CT scanners, and results in measurements from a dynamic imaging technique. Further, the approach is non-invasive, quantitative, and will meet the critical need for evidence-based, diagnostic information in the early stages of the continuum of wrist instability, which is known to progress to the development of wrist osteoarthritis.

Acknowledgment

The authors would like to recognize Matthew Koff, Ph.D., for his assistance with proximity mapping algorithms.

The project described was supported by Award No. R21 AR 057902 from the National Institute of Arthritis and Musculoskeletal and Skin Diseases, and Award No. T32 HD 07447 from the National Institute of Child Health and Human Development. The study sponsors had no role in study design, collection, analysis, or interpretation of the data, in the writing of the manuscript, or in the decision to submit this manuscript for publication.

References

[1] Garcia-Elias, M., and Folgar, M. A., 2006, "The Management of Wrist Injuries: An International Perspective," Injury, **37**(11), pp. 1049–1056.
[2] Guly, H. R., 2002, "Injuries Initially Misdiagnosed as Sprained Wrist (Beware the Sprained Wrist)," Emerg. Med. J., **19**(1), pp. 41–42.
[3] Jones, W. A., 1988, "Beware the Sprained Wrist: The Incidence and Diagnosis of Scapholunate Instability," J. Bone Jt. Surg., Br., **70**(2), pp. 293–297.
[4] Minami, A., Kato, H., and Iwasaki, N., 2003, "Treatment of Scapholunate Dissociation: Ligamentous Repair Associated With Modified Dorsal Capsulodesis," Hand Surg., **8**(1), pp. 1–6.
[5] O'Meeghan, C. J., Stuart, W., Mamo, V., Stanley, J. K., and Trail, I. A., 2003, "The Natural History of an Untreated Isolated Scapholunate Interosseus Ligament Injury," J. Hand Surg. Br., **28**(4), pp. 307–310.
[6] Watson, H., Ottoni, L., Pitts, E. C., and Handal, A. G., 1993, "Rotary Subluxation of the Scaphoid: A Spectrum of Instability," J. Hand Surg. Br., **18**(1), pp. 62–64.
[7] Watson, H. K., and Ballet, F. L., 1984, "The SLAC Wrist: Scapholunate Advanced Collapse Pattern of Degenerative Arthritis," J. Hand Surg. Am., **9**(3), pp. 358–365.
[8] Watson, H. K., Weinzweig, J., and Zeppieri, J., 1997, "The Natural Progression of Scaphoid Instability," Hand Clin., **13**(1), pp. 39–49.
[9] Rominger, M. B., Bernreuter, W. K., Kenney, P. J., and Lee, D. H., 1993, "MR Imaging of Anatomy and Tears of Wrist Ligaments," Radiographics, **13**(6), pp. 1233–1246 (Discussion 1247–1248).
[10] Schadel-Hopfner, M., Iwinska-Zelder, J., Braus, T., Bohringer, G., Klose, K. J., and Gotzen, L., 2001, "MRI Versus Arthroscopy in the Diagnosis of Scapholunate Ligament Injury," J. Hand Surg. Br., **26**(1), pp. 17–21.
[11] Braunstein, E. M., Louis, D. S., Greene, T. L., and Hankin, F. M., 1985, "Fluoroscopic and Arthrographic Evaluation of Carpal Instability," AJR, Am. J. Roentgenol., **144**(6), pp. 1259–1262.
[12] Gilula, L. A., Hardy, D. C., Totty, W. G., and Reinus, W. R., 1987, "Fluoroscopic Identification of Torn Intercarpal Ligaments After Injection of Contrast Material," AJR, Am. J. Roentgenol., **149**(4), pp. 761–764.
[13] White, S. J., Louis, D. S., Braunstein, E. M., Hankin, F. M., and Greene, T. L., 1984, "Capitate-Lunate Instability: Recognition by Manipulation Under Fluoroscopy," AJR, Am. J. Roentgenol., **143**(2), pp. 361–364.
[14] Beek, M., Small, C. F., Csongvay, S., Sellens, R. W., Ellis, R. E., and Pichora, D. R., 2004, "Wrist Kinematics From Computed Tomography Data," *Medical Image Computing and Computer-Assisted Intervention–MICCAI 2004*, Vol. 3217, C. Barillot, D. R. Haynor, and P. Hellier, eds., Springer-Verlag, Saint-Malo, France, pp. 1040–1041.
[15] Crisco, J. J., Coburn, J. C., Moore, D. C., Akelman, E., Weiss, A. P., and Wolfe, S. W., 2005, "In Vivo Radiocarpal Kinematics and the Dart Thrower's Motion," J. Bone Jt. Surg. Am., **87**(12), pp. 2729–2740.
[16] Crisco, J. J., Wolfe, S. W., Neu, C. P., and Pike, S., 2001, "Advances in the In Vivo Measurement of Normal and Abnormal Carpal Kinematics," Orthop. Clin. North Am., **32**(2), pp. 219–231.
[17] Feipel, V., and Rooze, M., 1999, "Three-Dimensional Motion Patterns of the Carpal Bones: An In Vivo Study Using Three-Dimensional Computed Tomography and Clinical Applications," Surg. Radiol. Anat., **21**(2), pp. 125–131.
[18] Goto, A., Moritomo, H., Murase, T., Oka, K., Sugamoto, K., Arimura, T., Masumoto, J., Tamura, S., Yoshikawa, H., and Ochi, T., 2005, "In Vivo Three-Dimensional Wrist Motion Analysis Using Magnetic Resonance Imaging and Volume-Based Registration," J. Orthop. Res., **23**(4), pp. 750–756.
[19] Ishikawa, J., Cooney, W. P., 3rd, Niebur, G., An, K. N., Minami, A., and Kaneda, K., 1999, "The Effects of Wrist Distraction on Carpal Kinematics," J. Hand Surg. Am., **24**(1), pp. 113–120.
[20] Kobayashi, M., Berger, R. A., Nagy, L., Linscheid, R. L., Uchiyama, S., Ritt, M., and An, K. N., 1997, "Normal Kinematics of Carpal Bones: A Three-Dimensional Analysis of Carpal Bone Motion Relative to the Radius," J. Biomech., **30**(8), pp. 787–793.
[21] Moojen, T. M., Snel, J. G., Ritt, M. J., Kauer, J. M., Venema, H. W., and Bos, K. E., 2002, "Three-Dimensional Carpal Kinematics In Vivo," Clin. Biomech., **17**(7), pp. 506–514.
[22] Moritomo, H., Murase, T., Goto, A., Oka, K., Sugamoto, K., and Yoshikawa, H., 2004, "Capitate-Based Kinematics of the Midcarpal Joint During Wrist Radioulnar Deviation: An In Vivo Three-Dimensional Motion Analysis," J. Hand Surg. Am., **29**(4), pp. 668–675.
[23] Patterson, R. M., Williams, L., Andersen, C. R., Koh, S., and Viegas, S. F., 2007, "Carpal Kinematics During Simulated Active and Passive Motion of the Wrist," J. Hand Surg. Am., **32**(7), pp. 1013–1019.
[24] Short, W. H., Werner, F. W., Fortino, M. D., and Mann, K. A., 1997, "Analysis of the Kinematics of the Scaphoid and Lunate in the Intact Wrist Joint," Hand Clin., **13**(1), pp. 93–108.
[25] Werner, F. W., Green, J. K., Short, W. H., and Masaoka, S., 2004, "Scaphoid and Lunate Motion During a Wrist Dart Throw Motion," J. Hand Surg. Am., **29**(3), pp. 418–422.
[26] Berdia, S., Short, W. H., Werner, F. W., Green, J. K., and Panjabi, M., 2006, "The Hysteresis Effect in Carpal Kinematics," J. Hand Surg. Am., **31**(4), pp. 594–600.
[27] Berger, R. A., 1997, "The Ligaments of the Wrist. A Current Overview of Anatomy With Considerations of Their Potential Functions," Hand Clin., **13**(1), pp. 63–82.
[28] Berger, R. A., Imaeda, T., Berglund, L., An, K. N., Cooney, W. P., Amadio, P. C., and Linscheid, R. L., 1994, "The Anatomic, Constraint and Material Properties of the Scapholunate Interosseous Ligament: A Preliminary Study," *Advances in the Biomechanics of the Hand and Wrist* (NATO ASI Series, Vol. A 256), F. Schuind, K. N. An, W. P. Cooney, III, and M. Garcia-Elias, eds., Plenum Press, New York.
[29] Berger, R. A., Imaeda, T., Berglund, L. J., and An, K. N., 1999, "Constraint and Material Properties of the Subregions of the Scapholunate Interosseous Ligament," J. Hand Surg. Am., **24**(5), pp. 953–962.
[30] Jantea, C., An, K., Linscheid, R., and Cooney, W., 1994, "The Role of the Scapho-Trapezial-Trapezoidal Ligament Complex on Scaphoid Kinematics," *Advances in the Biomechanics of the Hand and Wrist*, Plenum Press, New York.
[31] Mitsuyasu, H., Patterson, R. M., Shah, M. A., Buford, W. L., Iwamoto, Y., and Viegas, S. F., 2004, "The Role of the Dorsal Intercarpal Ligament in Dynamic and Static Scapholunate Instability," J. Hand Surg. Am., **29**(2), pp. 279–288.
[32] Nagao, S., Patterson, R. M., Buford, W. L., Jr., Andersen, C. R., Shah, M. A., and Viegas, S. F., 2005, "Three-Dimensional Description of Ligamentous Attachments Around the Lunate," J. Hand Surg. Am., **30**(4), pp. 685–692.
[33] Ruby, L. K., An, K. N., Linscheid, R. L., Cooney, W. P., 3rd, and Chao, E. Y., 1987, "The Effect of Scapholunate Ligament Section on Scapholunate Motion," J. Hand Surg. Am., **12**(5 Pt 1), pp. 767–771.
[34] Crisco, J. J., Pike, S., Hulsizer-Galvin, D. L., Akelman, E., Weiss, A. P. C., and Wolfe, S. W., 2003, "Carpal Bone Postures and Motions are Abnormal in Both Wrists of Patients With Unilateral Scapholunate Interosseous Ligament Tears," J. Hand Surg. Am., **28**(6), pp. 926–937.
[35] Picha, B. M., Konstantakos, E. K., and Gordon, D. A., 2012, "Incidence of Bilateral Scapholunate Dissociation in Symptomatic and Asymptomatic Wrists," J. Hand Surg. Am., **37**(6), pp. 1130–1135
[36] Choi, Y. S., Lee, Y. H., Kim, S., Cho, H. W., Song, H. T., and Suh, J. S., 2013, "Four-Dimensional Real-Time Cine Images of Wrist Joint Kinematics Using Dual Source CT With Minimal Time Increment Scanning," Yonsei Med. J., **54**(4), pp. 1026–1032.
[37] Demehri, S., Wadhwa, V., Thawait, G. K., Fattahi, N., Means, K. R., Carrino, J. A., and Chhabra, A., 2014, "Dynamic Evaluation of Pisotriquetral Instability Using 4-Dimensional Computed Tomography," J. Comput. Assisted Tomogr., **38**(4), pp. 507–512.

[38] Edirisinghe, Y., Troupis, J. M., Patel, M., Smith, J., and Crossett, M., 2014, "Dynamic Motion Analysis of Dart Throwers Motion Visualized Through Computerized Tomography and Calculation of the Axis of Rotation," J. Hand Surg. Eur., **39**(4), pp. 364–372.
[39] Garcia-Elias, M., Alomar Serrallach, X., and Monill Serra, J., 2014, "Dart-Throwing Motion in Patients With Scapholunate Instability: A Dynamic Four-Dimensional Computed Tomography Study," J. Hand Surg. Eur., **39**(4), pp. 346–352.
[40] Goh, Y. P., and Lau, K. K., 2012, "Using the 320-Multidetector Computed Tomography Scanner for Four-Dimensional Functional Assessment of the Elbow Joint," Am. J. Orthop., **41**(2), pp. E20–E24.
[41] Halpenny, D., Courtney, K., and Torreggiani, W. C., 2012, "Dynamic Four-Dimensional 320 Section CT and Carpal Bone Injury: A Description of a Novel Technique to Diagnose Scapholunate Instability," Clin. Radiol., **67**(2), pp. 185–187.
[42] Shores, J. T., Demehri, S., and Chhabra, A., 2013, "Kinematic '4 Dimensional' CT Imaging in the Assessment of Wrist Biomechanics Before and After Surgical Repair," ePlasty, **13**, p. e9.
[43] Wassilew, G. I., Janz, V., Heller, M. O., Tohtz, S., Rogalla, P., Hein, P., and Perka, C., 2013, "Real Time Visualization of Femoroacetabular Impingement and Subluxation Using 320-Slice Computed Tomography," J. Orthop. Res., **31**(2), pp. 275–281.
[44] Leng, S., Zhao, K., Qu, M., An, K. N., Berger, R., and Mccollough, C. H., 2011, "Dynamic CT Technique for Assessment of Wrist Joint Instabilities," Med. Phys., **38**(Suppl. 1), p. S50.
[45] Biswas, D., Bible, J. E., Bohan, M., Simpson, A. K., Whang, P. G., and Grauer, J. N., 2009, "Radiation Exposure From Musculoskeletal Computerized Tomographic Scans," J. Bone Jt. Surg. Am., **91**(8), pp. 1882–1889.
[46] Schauer, D., 2009, "Ionizing Radiation Exposure of the Population of the United States," The National Council on Radiation Protection and Measurements (NCRP), Report No. 160.
[47] Sebastian, T. B., Tek, H., Crisco, J. J., and Kimia, B. B., 2003, "Segmentation of Carpal Bones From CT Images Using Skeletally Coupled Deformable Models," Med. Image Anal., **7**(1), pp. 21–45.
[48] Salembier, P., and Serra, J., 1995, "Flat Zones Filtering, Connected Operators, and Filters by Reconstruction," IEEE Trans. Image Process., **4**(8), pp. 1153–1160.
[49] Meyer, F., and Beucher, S., 1990, "Morphological Segmentation," J. Visual Commun. Image Representation, **1**(1), pp. 21–46.
[50] Lorensen, W. E., and Cline, H. E., 1987, "Marching Cubes: A High Resolution 3D Surface Construction Algorithm," ACM Comput. Graphics, **21**(4), pp. 163–169.
[51] Lin, W. T., and Robb, R. A., 2000, "Patient Specific Physics-Based Model for Interactive Visualization of Cardiac Dynamics," Stud. Health Technol. Inf., **70**, pp. 182–188.
[52] Eusemann, C. D., Bellemann, M. E., and Robb, R. A., 2000, "Measurement and Display of Instantaneous Regional Motion of the Myocardium," Proc. SPIE **3911**, pp. 34–41.
[53] Haider, C. R., Bartholmai, B. J., Holmes, D. R., Camp, J. J., and Robb, R. A., 2005, "Quantitative Characterization of Lung Disease," Comput. Med. Imaging Graphics, **29**(7), pp. 555–563.
[54] Besl, P. J., and Mckay, N. D., 1992, "A Method for Registration of 3-D Shapes," IEEE Trans. Pattern Anal. Mach. Intell., **14**(2), pp. 239–256.
[55] Hansson, G.-A., Balogh, I., Ohlsson, K., Granqvist, L., Nordander, C., Arvidsson, I., Akesson, I., Unge, J., Rittner, R., Stromberg, U., and Skerfving, S., 2009, "Physical Workload in Various Types of Work: Part I: Wrist and Forearm," Int. J. Ind. Ergon., **39**(1), pp. 221–233.
[56] Bey, M. J., Kline, S. K., Tashman, S., and Zauel, R., 2008, "Accuracy of Biplane X-Ray Imaging Combined With Model-Based Tracking for Measuring In-Vivo Patellofemoral Joint Motion," J. Orthop. Surg. Res., **3**, p. 38.
[57] Crisco, J. J., McGovern, R. D., and Wolfe, S. W., 1999, "Noninvasive Technique for Measuring In Vivo Three-Dimensional Carpal Bone Kinematics," J. Orthop. Res., **17**(1), pp. 96–100.
[58] Miranda, D. L., Schwartz, J. B., Loomis, A. C., Brainerd, E. L., Fleming, B. C., and Crisco, J. J., 2011, "Static and Dynamic Error of a Biplanar Videoradiography System Using Marker-Based and Markerless Tracking Techniques," ASME J. Biomech. Eng., **133**(12), p. 121002.
[59] Tashman, S., and Anderst, W., 2003, "In-Vivo Measurement of Dynamic Joint Motion Using High Speed Biplane Radiography and CT: Application to Canine ACL Deficiency," ASME J. Biomech. Eng., **125**(2), pp. 238–245.
[60] Mak, W. H., Szabo, R. M., and Myo, G. K., 2012, "Assessment of Volar Radiocarpal Ligaments: MR Arthrographic and Arthroscopic Correlation," Am. J. Roentgenol., **198**(2), pp. 423–427.